ZnO THIN FILMS PREPARED BY SPRAY-PYROLYSIS TECHNIQUE FROM ORGANO-METALLIC PRECURSOR

#LADISLAV NÁDHERNÝ, ZDENĚK SOFER, DAVID SEDMIDUBSKÝ, ONDŘEJ JANKOVSKÝ, MARTIN MIKULICS*

Department of Inorganic Chemistry, Institute of Chemical Technology, Technická 5, 166 28 Prague 6, Czech Republic
**Peter Grünberg Institute (PGI-9), Forschungszentrum Jülich, D-52425 Jülich, Germany*

#E-mail: ladislav.nadherny@vscht.cz

Submitted March 10, 2012; accepted May 6, 2012

Keywords: Zinc oxide, Thin films, Spray-pyrolysis, Zinc acetyl-acetonate

Presented experiments utilize methanolic solution of zinc acetyl-acetonate as a precursor and sapphire (001) as a substrate for deposition of thin films of ZnO. The X-ray diffraction analysis revealed polycrystalline character of prepared films with preferential growth orientation along c-axis. The roughness of prepared films was assessed by AFM microscopy and represented by roughness root mean square (RMS) value in range of 1.8 - 433 nm. The surface morphology was mapped by scanning electron microscopy showing periodical structure with several local defects. The optical transmittance spectrum of ZnO films was measured in wavelength range of 200-1000 nm. Prepared films are transparent in visible range with sharp ultra-violet cut-off at approximately 370 nm. Raman spectroscopy confirmed wurtzite structure and the presence of compressive stress within its structure as well as the occurrence of oxygen vacancies. The four-point Van der Pauw method was used to study the transport prosperities. The resistivity of presented ZnO films was found 8 × 10^{-2} Ω cm with carrier density of 1.3 × 10^{18} cm^{-3} and electron mobility of 40 cm^2 V^{-1} s^{-1}.

INTRODUCTION

Zinc oxide is due to its extraordinary properties a very promising semiconducting material used in many branches. ZnO belongs to the group $A^{II}B^{VI}$ semiconductors and it reveals the broadest band gap (3.437 eV at 2 K [1] and 3.36 eV at room temperature) and largest exciton binding energy (60 mV) among the members of this group [1-4]. Such parameters are important for applications in optics [5, 6], where the zinc oxide is used as a component for UV and blue range, and also as an optical waveguide [7], photocatalyst [8], or solar cells window [9-11]. Furthermore the manufacture of zinc oxide in a form of piezoelectric transducers, varistors, phosphorescent substances, transparent conductive films, transistors TFT (thin film transistors) or gas sensors has been also reported [12-14]. Zinc oxide resists better than Si or GaAs to radiation damage so its potential application in space is possible [1].

For the vast majority of applications ZnO is used in a form of thin films. Such films can be prepared by various deposition techniques. It could be chemical vapor deposition [15], spray pyrolysis [16, 17], spin-coating [18], dip-coating [19], magnetron sputtering [20], pulsed laser deposition (PLD) [21] or molecular beam epitaxy (MBE) [22].

Spray pyrolysis represents a perspective deposition method due to its technical simplicity, low-cost operation and the possibility of large-scale fabrication of thin films. There is also no extra demand to the ultra-high vacuum during the deposition process – layers can be prepared at medium-low or atmospheric pressure.

For gaseous phase deposition organo-metallic precursors are mostly used. Here are the most frequently used precursors: carbon-metal precursors [23], zinc-(II) salts [12, 24] or beta-diketonates of transition metals [25]. Acetyl-acetonates possess suitable characteristics for a deposition – high vapor pressure, low temperature decomposition and it is also non-toxic and environment friendly.

We thus used spray pyrolysis as a deposition method in this work. Structural quality of final films was examined and the morphological, optical, electrical, spectroscopic properties of ZnO films as functions of deposition temperature and pressure, liquid precursor flow, carrier gas flow and the inert and reactive gas ratio were studied.

EXPERIMENTAL

Pure ZnO thin films were deposited in horizontal quartz reactor on sapphire (001) substrate at a pressure from 25 to 75 kPa. Substrates were mounted on a Hastelloy C22 susceptor, which was inductively heated to the temperature in the range of 610 and 750 °C. Before

deposition, the substrates were cleaned with piranha solution [26] and rinsed in pure deionized water and blow-dried with pure nitrogen.

Zinc acetyl-acetonate dissolved in methanol was used as a precursor. Liquid flow controller was applied for dosage of precursor in the range of 20 and 30 $cm^3 h^{-1}$. Before entering the reactor, the solution of precursor was filtered by 2-μm porosity filter to prevent contamination by dust and possible formation of clots from precursor solution. Distribution of precursor solution and methanolic purge was made of Teflon tubing system equipped with electromagnetic valves with very low internal volume. This technology allows switching between multiple precursors and the possibility to grow heterostructures with relatively sharp interfaces. Stainless steel containers are pressurized by nitrogen to ensure a sufficient pressure gradient on liquid flow controller. The vacuum system was equipped with butterfly valve pressure stabilization system and two-stage rotary oil pump. An electromagnetic shut-off valve and relief vessel intended for freeze drying unreacted precursors and reaction products was placed prior to the pump.

In the beginning of each deposition process the reactor was completely exhausted and then the controlled flow rate of argon and oxygen mixture was introduced into the reactor.

The liquid precursor was injected by an ultrasonic atomizer into the reactor inlet. Resulting aerosol was carried by carrier gas to the input part of the reactor, whose temperature was controlled in the range of 170 and 210 °C. As a carrier gas a mixture of argon and oxygen was used, with a maximum oxygen concentration of 17%. Various concentration ratios of oxygen and argon were probed. Total gas flow was set up to 2400 $cm^3 min^{-1}$ and the deposition time was set to 40 minutes. The effect of reactor temperature and pressure, precursor liquid flow, total gas flow and the oxygen/argon ratio on the resulting structural quality of final layers were investigated.

Using the X-ray diffraction analysis the crystal structure of the prepared layers (including Omega scan) was determined. For X-ray diffraction Cu-Kα radiation with a wavelength λ = 1.5406 nm in Bragg-Brentano geometry was used. The optical microscopy (disposing by DIC contrast), AFM in tapping mode and SEM was applied for the surface morphology examination.

Electrical properties – resistivity, concentration of free carriers and mobility – of the prepared films were measured by a four-point Van der Pauw method at room temperature using indium contacts in magnetic field up to 0.5 T. Raman spectroscopy was performed on a confocal Raman microscope Renishaw inVia equipped with Nd-YAG laser at a wavelength of 532 nm and output of 50 mW. The UV-Vis transmittance spectra of prepared films were measured using Avantes spectrophotometer with 75 mm focal length diffractometer in the wavelength range from 200 to 1000 nm. The concentration of zinc in the precursor solution was determined by AAS spectroscopy (flame mode).

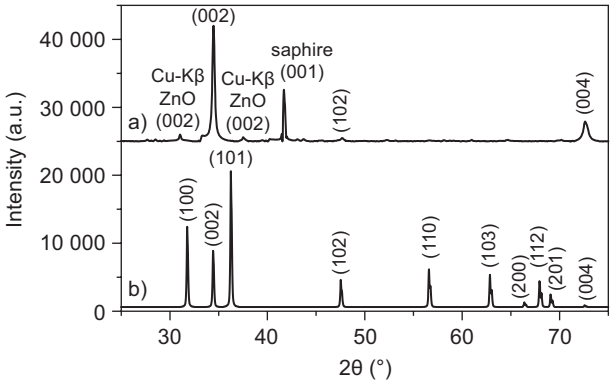

Figure 1. XRD diffractogram of a) thin film of ZnO and b) bulk ZnO (reference pattern PDF 01-075-0576).

RESULTS AND DISCUSSION

The influence of deposition parameters on the quality of the resulting layers was investigated. In particular the influence of the temperature and the pressure in the deposition reactor was examined. Besides, the precursor liquid flow, the total gas flow and the ratio of carrier gas and reaction gas effects on final film, were also studied. Figure 1 shows the comparison of ZnO powder diffractogram (reference database pattern) and the diffractogram of ZnO thin films deposited on sapphire substrate. The prepared films are textured and polycrystalline with high preferential orientation in (0 0 2) direction, that is in coherence with authors [11, 27-29]. The major peak at 2θ = 34.47° is a (0 0 2) reflection of zinc oxide while the peak at 2θ = 41.75° originates from the underlying sapphire substrate. Two small peaks at the angles of 2θ = 72.73° and 47.57°are ZnO reflections (0 0 4) and (1 0 2) respectively, that are visible due to the polycrystalline character of the deposited layers. Apparently the films grow preferentially along c-axis, in vertical direction to the substrate.

Due to the differences in lattice parameters of zinc oxide and sapphire, the layers contain significant concentration of defects and dislocations. The deposition performed at the temperature of 610 °C or 750 °C led to an enhanced surface roughness. The smoothest layer surface was prepared at the optimum temperature of 650 °C. Moreover, the layers prepared at this temperature grew with the highest achievable growth rate. The variation of surface roughness and growth rate can be attributed to the different thickness of substrate surface boundary layer and diffusion rate of precursors to the substrate surface trough the boundary layer. In the first series of layers deposition, when the temperature in the reactor was studied as a variable parameter, the films prepared at temperature of 650 °C, were found to exhibit the lowest

surface roughness, referring to the RMS = 10.5 nm. Once the temperature was lowered to 610 °C the RMS value increased to 12.6 nm. Layers deposited at 750 °C revealed a have very coarse surface (RMS = 101 nm). The surface morphology of the layers prepared at different temperatures is shown in Figure 2.

We assume that the increasing temperature also accelerates the decomposition reaction of the precursor and consequently faster growth of film grains. At low temperatures the resulting higher surface roughness can be caused by slow diffusion length of adsorbed reactants on the layer surface. The pressure increase in deposition reactor involves an enhancement of oxygen activity and promotes the grow rate of the layers. As a result, the increase of growth rate is also accompanied by a roughening of the layer surface. The surface morphology of the layer deposited at different pressures is shown in Figure 3. The higher growth rate also suppressed the diffusion length of adsorbed reactants and led to an increase of the surface roughness.

The lowest surface roughness RMS = 2.15 nm was achieved for the films prepared at 50 kPa. Both lowering pressure to 25 kPa and increasing in to 75 kPa had a negative influence on the surface roughness resulting in the respective values of RMS 51.2 and 433 nm.

Hence, in the next step, we used the deposition conditions 650 °C and 50 kPa. At higher flow rate the retention time of vapor precursor is reduced and as a consequence the growth rate is reduced. Another consequence is a more textured surface shown in Figure 4, which is probably due to the kinetic aspect of the deposition. Insufficient retention time in the reactor inlet led to an incomplete evaporation of the injected liquid precursor and to large concentration of macroscopic defects in the layer, which can be attributed to this effect.

At zero value of oxygen partial pressure the x-ray diffraction analysis shows only traces of polycrystalline zinc oxide. Substrate was colored dark gray, which probably indicates the formation of soot resulting from the decomposition of the organic matrix of precursor and

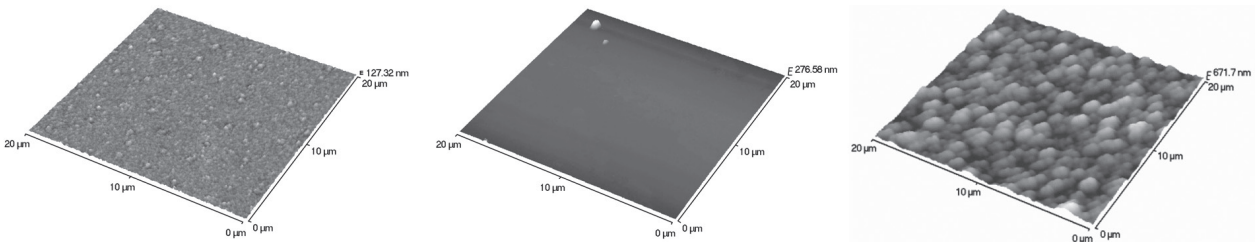

Figure 2. AFM images of thin films of ZnO prepared at temperature 610°C (left), 650°C (middle), 750°C (right).

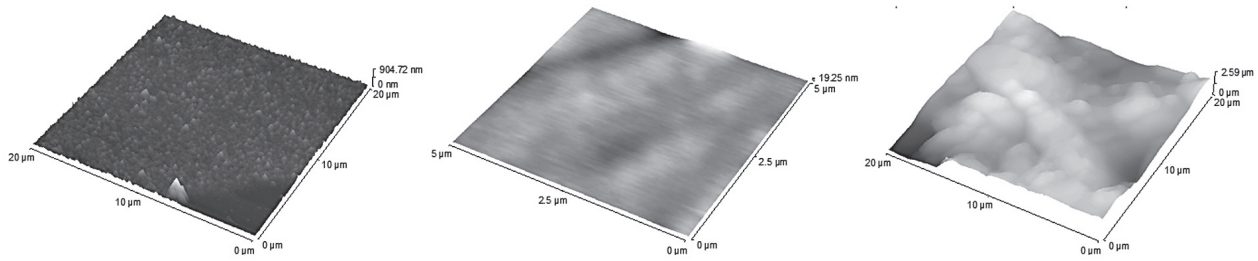

Figure 3. AFM images of thin films of ZnO prepared at 25 kPa (left), 50 kPa (middle) and 75 kPa (right).

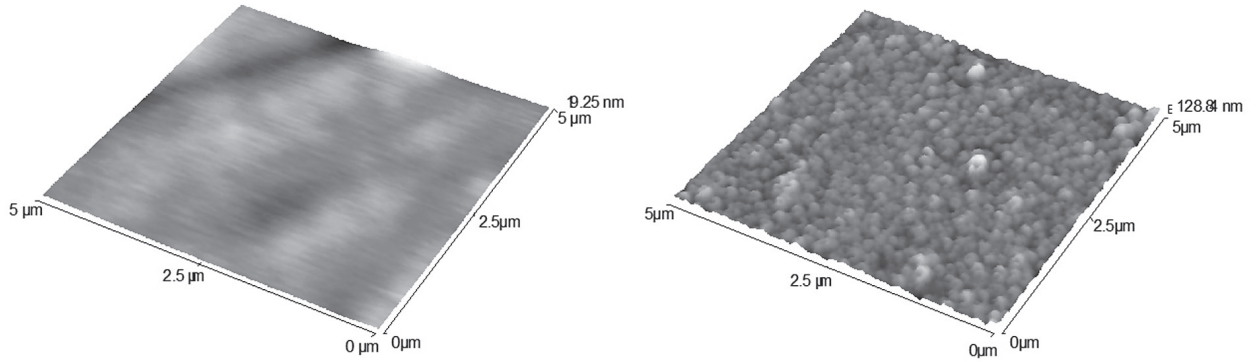

Figure 4. Shows almost perfectly smooth (RMS = 3.4 nm) layer surface of the sample deposited at precursor flow 20 cm^3 h^{-1} (left), in contrast to the film prepared with precursor flow of 30 cm^3 h^{-1} (right, RMS = 13.5 nm).

methanol (solvent) in the atmosphere of pure argon. In cases where the amount of oxygen was 17 %, the decomposition took place too exothermically – the predominant majority of the precursor reacted with oxygen before reaching the deposition part of the reactor. The resulting ZnO particles formed from decomposed zinc precursor led to high reduction of vaporized precursor partial pressure and subsequently to the reduction of growth rate. The optimal oxygen concentration of 14 % in carrier gas was found. The surface roughness RMS = 2.2 nm and the FWHM of rocking curve from (002) reflection was about 2700 arc sec.

The total carrier gas flow was studied in the range 600 – 2400 cm^3 min^{-1}. Other parameters were set constant (reactor pressure set to 500 mbar, the substrate was heated to 650 °C, precursor flow was 20 cm^3 h^{-1} and oxygen concentration in deposition chamber was 14 %). Decreasing the total flow of gaseous components to 600 cm^3 min^{-1} was likely causing a longer retention of vaporized precursor above the substrate and led to an increased growth of ZnO layers. However the surface roughness was substantially increased (RMS = 130 nm). In contrast, high flow rate (2400 cm^3 min^{-1}) also led to a roughening of the surface layers and to poorer structural quality manifested by a polycrystalline character with slight preferential orientation in (002) direction. Smoothest layers were prepared at the total flow rate of 1200 cm^3 min^{-1} with roughness RMS = 1.84 nm. Three representative films are shown in Figure 5.

UV-Vis transmittance of the prepared films was investigated in the wavelength range 200 – 1000 nm. In Figure 6 a 25 % transparency in the visible range is demonstrated. The lower throughput level is probably caused by defects of layers and dimness of the surface caused by analytical primary beam scattering. The spectral cut-off was observed at approximately 370 nm, which is consistent with other studies [5, 13]. The spectral edge wavelength corresponds to the energy gap E_g = 3.35 eV, which is slightly higher than that previously reported 3.2 eV [30]. Another research group presented the value 3.26 eV [25].

In the following paragraph we present Raman scattering in ZnO deposited layers with assigning detected peaks of particular energy modes.

Raman spectrum of pure ZnO measured at room temperature is shown in Figure 7. Peaks at 333 cm^{-1}, 440 cm^{-1}, 582 cm^{-1}, 792 cm^{-1} belong to ZnO, while all other peaks are related to the sapphire substrate. First, the middle-small band from low-wave number region at 333 cm^{-1} having acoustic combination is related to E_2^{high} – E_2^{low} process. The E_2 vibration mode at 440 cm^{-1} is characteristic of the wurtzite phase [31]. No shift of this E_2 vibration mode compared to unstrained single ZnO crystal was observed. The strain relaxation is accompanied by the formation of screw and mixed type of dislocations. The middle-weak peak at 582 cm^{-1} (sometimes occurred at 590 or 594 cm^{-1}) is related to the lattice defects, such as oxygen vacancy or interstitial zinc atoms in ZnO matrix [31, 32]. The presence of these defects and dislocations was proofed also by X-ray diffraction analysis by measurement of rocking curve from (002) reflection.

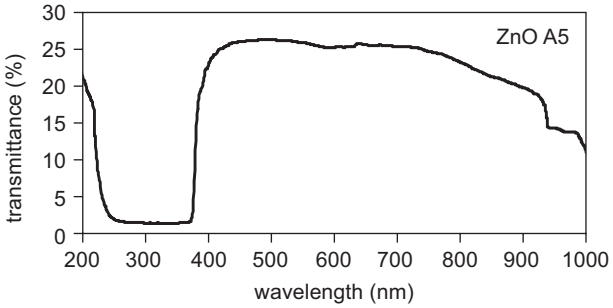

Figure 6. UV-Vis spectrum of ZnO thin film.

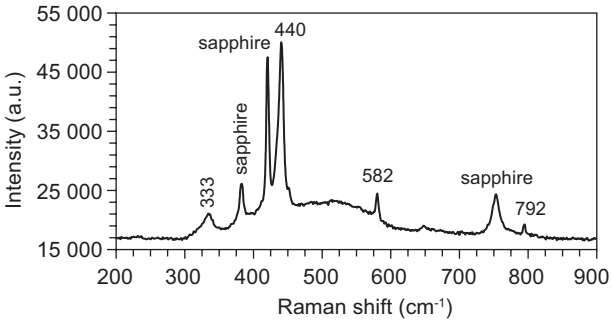

Figure 7. Raman spectrum of pure ZnO thin film excited by 532 nm Nd-YAG laser.

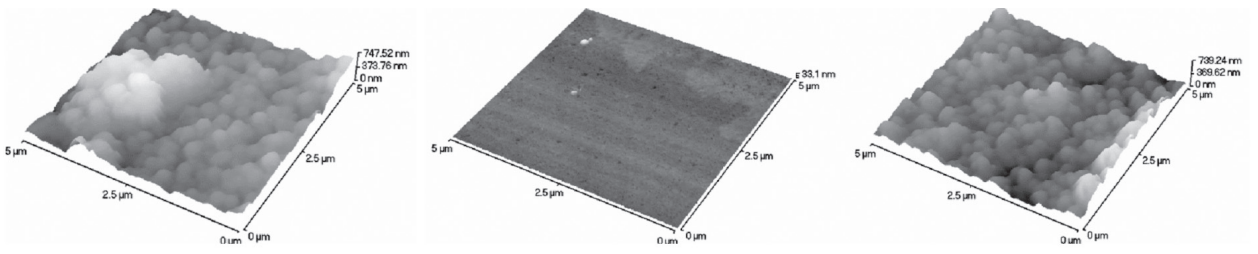

Figure 5. AFM images of ZnO thin films prepared at various total gas flow; 600 cm^3 min^{-1} on the left (RMS = 130 nm), 1200 cm^3 min^{-1} in the middle (RMS = 1.84 nm) and 2400 cm^3 min^{-1} on the right (RMS = 102 nm).

The small peak at 792 cm^{-1} belonging to the high-wave number region (700 – 1200 cm^{-1}) is connected with overtones, acoustic and optical combinations and describes longitudinal acoustic and transversal optic process. [32]
ZnO transversal modes at 380 cm and 408 cm^{-1} [31] are probably covered by sapphire signal.

The resistivity of undoped ZnO thin films was reported in the range of 1×10^{-3} and 1×10^{2} Ω cm [11, 28, 33]. The high dispersion of the reported values is associated mainly with the different oxygen partial pressure during the deposition process. The oxygen vacancies in ZnO thin films are responsible for n-type conductivity in case of undoped ZnO thin films and broad variation of resistivity. The resistivity of thin films from spray pyrolysis growth was measured in the range of 0.05 to 0.1 Ω cm. Very low values of resistivity are associated with high concentration of oxygen vacancies which was observed also by Raman spectroscopy. The layers exhibit pure n-type conductivity. Free carrier concentration was 1.3×10^{18} cm^{-3} which is comparable with other reported measurements on highly conductive zinc oxide thin films [16, 33]. The free carrier mobility was in the range of 20 to 40 $cm^2 V^{-1} s^{-1}$.

CONCLUSION

The thin films of ZnO were prepared using spray pyrolysis technique and Zn-acetyl-acetone in argon-oxygen atmosphere. The influence of deposition parameters affecting the quality and properties of the resulting films was investigated. The studied parameters were temperature and pressure in the deposition reactor, liquid flow precursor dosage, the total gas flow and the partial pressure of reaction gas. For the thin films grown with optimized conditions, the value of FWHM from Omega-scan was below 1500 arc sec and the roughness from AFM microscopy expressed as RMS was below 2 nm (for an area of 25 nm^2). The films are reasonably transparent in visible range with resulted the band gap of 3.35 eV. Raman investigation of prepared ZnO thin films confirmed the wurtzite structure and the oxygen vacancies due to the low oxygen partial pressure during the deposition process. The films exhibit pure n-type conductivity with resistivity in the range of 0.05 and 0.1 Ω cm. The highest electron mobility measured on the films was 40 $cm^2 V^{-1} s^{-1}$ with carrier concentration of 1.3×10^{18} cm^{-3}.

Acknowledgements

This project was supported by the Czech Science Foundation (grant N° 104/09/0621), by ICT Prague (project N° A1_FCHT_2012_006) and by Ministry of Education of the Czech Republic (specific university research MSMT 21/2012).

References

1. Look D. C.: Mater. Sci. Eng. B *80*, 383 (2001).
2. Ozgur U., Alivov Y. I., Liu C., Teke A., Reshchikov M.A., Dogan S., Avrutin V., Cho S.J., Morkoc H.: J. Appl. Phys. *98*, 1 (2005).
3. Triboulet R., Perrière J.: Prog. Cryst. Growth Charact. Mater. *47*, 65 (2003).
4. Kirchner C., Gruber T., Reuß F., Thonke K., Waag A., Gießen C., Heuken M.: J. Cryst. Growth. *248*, 20 (2003).
5. Achour Z.B., Ktari T., Ouertani B., Touayar O., Bessais B., Brahim J.B.: Sens. Actuators A *134*, 447 (2007).
6. Janotti A., Van d. W.C.G.: Rep. Prog. Phys. *72*, 126501/1 (2009).
7. Ibanga E.J., Le Luyer C., Mugnier J.: Mater. Chem. Phys. *80*, 490 (2003).
8. Torres D.G., Zuniga R.C.I., Mayen H.S.A., Castanedo P.R., Zelaya A.O.: Sol. Energy Mater. Sol. Cells. *93*, 55 (2009).
9. Fay S., Shah A.: Springer Ser. Mater. Sci. *104*, 235 (2008).
10. Ellmer K., Klein A.: Springer Ser. Mater. Sci. *104*, 1 (2008).
11. Mohammad M.T., Hashim A.A., Al-Maamory M.H.: Mater. Chem. Phys. *99*, 382 (2006).
12. Shinde V.R., Gujar T.P., Lokhande C.D.: Sens. Actuators B. *120*, 551 (2007).
13. Kiriakidis G., Moschovis K., Kortidis I., Binas V.: Vacuum *86*, 495 (2012).
14. Wang, B., Min, J., Zhao, Y., Sang, W. and Wang, C.: Appl. Phys. Lett. *94*, 192101 (2009).
15. Li X., Yan Y., Gessert T.A., DeHart C., Perkins C.L., Young D., Coutts T.J.: Electrochem. Solid-State Lett. *6*, C56 (2003).
16. Yoshino K., Fukushima T., Yoneta M.: J. Mater. Sci.: Mater. Electron. *16*, 403 (2005).
17. Ayouchi R., Martin F., Leinen D., Ramos-Barrado J.R.: J. Cryst. Growth. *247*, 497 (2003).
18. Znaidi L.: Materials Science and Engineering: B *174*, 18 (2010).
19. Valle G.G., Hammer P., Pulcinelli S.H., Santilli C.V.: J. Eur. Ceram. Soc. *24*, 1009 (2004).
20. Ko H., Tai W.P., Kim K.C., Kim S.H., Suh S.J., Kim Y.S.: J. Cryst. Growth. *277*, 352 (2005).
21. Park S.M., Ikegami T., Ebihara K., Shin P.K.: Applied Surf. Sci. *253*, 1522 (2006).
22. Heo Y.W., Norton D.P., Pearton S.J.: J. Appl. Phys. *98*, 1 (2005).
23. Ma Y., Du G.T., Yang S.R., Li Z.T., Zhao B.J., Yang X.T., Yang T.P., Zhang Y.T., Liu D.L.: J. Appl. Phys. *95*, 6268 (2004).
24. Allah F.K., Abé S.Y., Núñez C.M., Khelil A., Cattin L., Morsli M., Bernède J.C., Bougrine A., del Valle M.A., Díaz F.R.: Applied Surf. Sci. *253*, 9241 (2007).
25. Khranovskyy V., Grossner U., Lazorenko V., Lashkarev G., Svensson B.G., Yakimova R.: Superlattices Microstruct. *39*, 275 (2006).
26. Douglass, K., Hunt, S., Teplyakov, A. and Opila, R. L.: Appl. Surf. Sci. *257*, 1469 (2010).
27. Pawar B.N., Jadkar S.R., Takwale M.G.: J. Phys. Chem. Solids. *66*, 1779 (2005).
28. Lokhande B.J., Patil P.S., Uplane M.D.: Mater. Lett. *57*, 573 (2002).
29. Gomez H., Maldonado A., Olvera M.D.L.L., Acosta D.R.: Sol. Energy Mater. Sol. Cells. *87*, 107 (2005).
30. Ayouchi R., Leinen D., Martín F., Gabas M., Dalchiele E., Ramos-Barrado J.R.: Thin Solid Films. *426*, 68 (2003).
31. Yahia S.B., Znaidi L., Kanaev A., Petitet J.P.: Spectrochim. Acta A *71*, 1234 (2008).
32. Shinde S.S., Shinde P.S., Sathe V.G., Barman S.R., Bhosale C.H., Rajpure K.Y.: J. Mol. Struct. *984*, 186 (2010).
33. Ma Y., Du G.T., Yang T.P., Qiu D.L., Zhang X., Yang H.J., Zhang Y.T., Zhao B.J., Yang X.T., Liu D.L.: J. Cryst. Growth. *255*, 303 (2003).